ACADEMIC PRESS

Available online at www.sciencedirect.com

SCIENCE DIRECT®

Journal of Sound and Vibration 261 (2003) 443–464

JOURNAL OF SOUND AND VIBRATION

www.elsevier.com/locate/jsvi

Finite element modelling for fatigue stress analysis of large suspension bridges

Tommy H.T. Chan[a,*], L. Guo[b], Z.X. Li[b]

[a] *Department of Civil and Structural Engineering, The Hong Kong Polytechnic University, Hung Hom, Kowloon, Hong Kong*

[b] *College of Civil Engineering, Southeast University, Nanjing 210096, China*

Received 9 January 2001; accepted 27 May 2002

Abstract

Fatigue is an important failure mode for large suspension bridges under traffic loadings. However, large suspension bridges have so many attributes that it is difficult to analyze their fatigue damage using experimental measurement methods. Numerical simulation is a feasible method of studying such fatigue damage. In British standards, the finite element method is recommended as a rigorous method for steel bridge fatigue analysis. This paper aims at developing a finite element (FE) model of a large suspension steel bridge for fatigue stress analysis. As a case study, a FE model of the Tsing Ma Bridge is presented. The verification of the model is carried out with the help of the measured bridge modal characteristics and the online data measured by the structural health monitoring system installed on the bridge. The results show that the constructed FE model is efficient for bridge dynamic analysis. Global structural analyses using the developed FE model are presented to determine the components of the nominal stress generated by railway loadings and some typical highway loadings. The critical locations in the bridge main span are also identified with the numerical results of the global FE stress analysis. Local stress analysis of a typical weld connection is carried out to obtain the hot-spot stresses in the region. These results provide a basis for evaluating fatigue damage and predicting the remaining life of the bridge.

1. Introduction

Fatigue is an important failure mode for steel structures. In fact, 80–90% of failures in steel structures are related to fatigue and fracture [1]. Nowadays, more and more large steel bridges are being constructed worldwide, and some are expected to be vulnerable to fatigue-related problems.

*Corresponding author. Tel.: +852-2766-6061; fax: +852-2334-6389.
E-mail address: cetommy@polyu.edu.hk (T.H.T. Chan).

0022-460X/03/$ - see front matter
PII: S0022-460X(02)01086-6

It is important to study fatigue damage in these bridges. Fatigue analysis for an existing bridge is predominantly based on stress analysis, to get the distribution of stress in structures. Recently, some important works on fatigue analysis for bridges have been found [4,5]. In those works, short- or medium-span bridges were the focus, and, the finite element method (FEM) was used to decide the critical locations due to fatigue damage. Field tests were then conducted for assessment of the stress range in these critical locations.

A long-suspension bridge is a very flexible and lightly damped structure. Heavy trucks and railway vehicles running on a long-suspension bridge may significantly change local dynamic behavior and affect the fatigue life of the bridge. Generally, a long-suspension bridge has a sheer size and is over water, which makes access for inspection, instrumentation and testing very difficult. Many experimental techniques that have been shown to be successful for structural identification of short- and medium-span bridges cannot simply be scaled-up to long-span bridges [2]. All of these factors make it very difficult to study fatigue damage in long-suspension bridges with experimental measurement. Correspondingly, numerical simulation is a feasible method to study such fatigue damage.

The FEM is recommended by the British standards [3] as a rigorous method for structural fatigue stress analysis. The studies [6,7] show that FEM has become a highly valuable tool as a basis for evaluation of fatigue behavior. The latest work by Lin and Smith [8–10] describes the finite element (FE) modelling of fatigue crack growth of surface cracked plates, and provides an accurate evaluation of the fatigue life of the structures. However, it is very complicated to establish a FE model of a large practical structure for fatigue damage analysis, as the FE model should embody the sectional properties of structural members. Moreover, in considering that fatigue damage is a local failure mode and often occurs in welded regions, the weld detail should also be included in the FE model. There is no related work found in literature about the study of fatigue damage of large suspension bridges using FEM, and therefore it becomes a significant problem to be studied.

The Tsing Ma Bridge (TMB), which is 2.2 km in total length and has a main span of 1377 m, as shown in Fig. 1, is the longest suspension bridge in the world, carrying both road and rail traffic. As the main part of the Lantau Link, a combined highway and railway transport connection between Tsing Yi Island and Lantau Island, it forms an essential part of the transport network for the new Hong Kong airport. In order to ensure user comfort and the safety of the TMB, a structural health monitoring system has been devised and installed to monitor the integrity, durability and reliability of the bridge. This monitoring system comprises a total of approximately 350 sensors, including accelerometers, strain gauges, displacement transducers, level sensors, anemometers, temperature sensors and weigh-in-motion (WIM) sensors, installed permanently on the bridge. The strain gauges were installed to measure stresses at bridge-deck sections. By use of the online strain time-history data, some important work [11,12] on the fatigue damage analysis and service life prediction of the bridge-deck section of the TMB has been carried out. However, the locations of the monitoring sensors setting in the bridge were selected for general purposes and such locations might not be critical to fatigue damage. The analysis of the TMB global dynamic response and the stress–time history under traffic loading in the members are needed. Moreover, if the bridge is subjected to some disastrous conditions, such as during or after an earthquake, the online data measured by the health monitor system will not be able to directly predict the degree of damage. In this paper, a large FE model of the TMB (depicted in Fig. 1(b)), embodying the

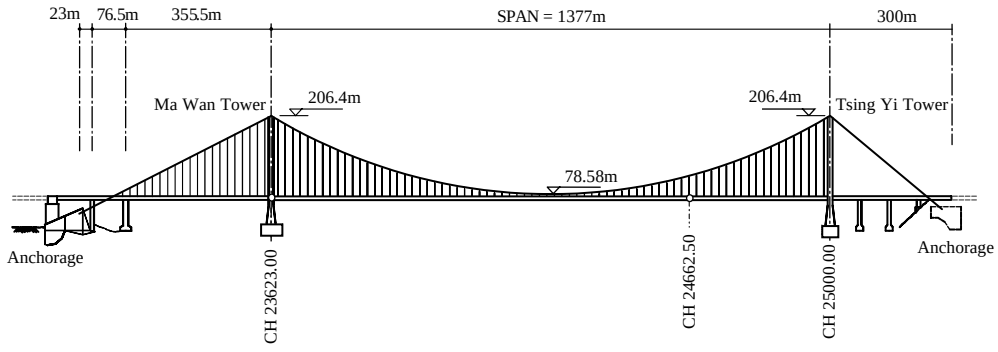

(a) sketch of Tsing Ma Bridge

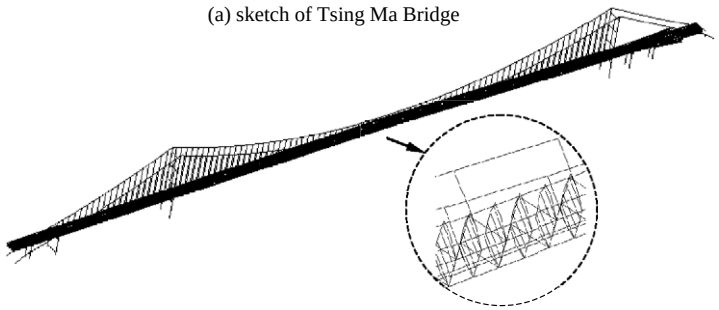

(b) FE model of Tsing Ma

Fig. 1. Configuration of the TMB and FE model.

properties of almost all the structural members, is developed. The welded regions are manifested by the relative mesh method. The dynamic characteristics of the TMB and its dynamic responses under traffic loading are studied with the established FE model. Comparisons of the computed results with the measured data are presented to demonstrate the validity, accuracy and capability of the proposed FEM. These results provide a basis of evaluating fatigue damage and predicting the remaining life of the TMB. Moreover, with the developed FE model, the dynamic responses of the bridge under a heavy traffic accident, typhoon attack, and/or earthquake could be simulated.

2. Fe model of the TMB

Bridge fatigue is a high-cycle fatigue problem where stress fluctuations are so low that the deformation in the structure is elastic except at notches and welded joints where local stresses are concentrated. Consequently, an elastic FE model was needed for global stress estimation of the bridge in virgin state due to traffic loading, so that critical locations due to fatigue damage could be identified. As shown in Fig. 1, the TMB is a double-deck suspension bridge. It contains about 20 000 structural members, including longitudinal trusses, cross-frames, deck plates, tower beams, main cables, hangers, etc. In recognizing that the conventional modelling procedure for cable supported bridges by approximating the bridge deck as analogous beams or grids is not applicable

for accurate fatigue stress analysis, a precise FE model of the TMB was developed using the commercial software package ABAQUS.

In the developed FE model, longitudinal trusses in the bridge deck, comprising chords, posts and diagonal bracings, were modelled as 3-D, two-node iso-parametric beam elements having six degrees of freedom (d.o.f.) at each node. Bending, torsional and axial force effects were all considered in each space beam element. The section details were also embodied in the corresponding elements: the top and bottom chords which are box section members, were modelled as space beam elements with box sections; vertical posts and, diagonal bracings were represented by space I-beam elements, as they are all fabricated H-sections. Considering their H-sections, cross-frames in the deck were also modelled as 3-D I-beam elements.

The main cables and hangers, generally simulated as truss elements, were still modelled as two-node space beam elements with circular cross-sections. Highway pavements were modelled by 3-D four-node doubly curved shell elements with reduced integration to control the hourglass. For convenient connection with the beam elements, the six d.o.f. at each node were also selected in the shell elements. Railway beams are made up of two inverted T-beams welded to flange plates. They act as continuous longitudinal beams supporting a track bed. Correspondingly, each rail track was represented by continuous beam elements with I-section. The Tsing Yi and Ma Wan Towers are made of reinforced concrete and are supported by hard foundations. They were modelled as rigid bodies. Some two-node flexible joint elements with six d.o.f. at each node were used to simulate the relative joint connections, such as bearings in the bridge deck. All of the corresponding element properties are listed in detail in Ref. [13].

It is complicated to simulate large practical structures such as the TMB. As the aforementioned analysis shows, the welded regions are vulnerable to fatigue damage. Therefore, an efficient FE model for fatigue analysis should be able to output the stress at these locations. When the stress histories in the elements around a welded connection were obtained, using a proposed local FE model described later in the paper, the hot-spot stress in the welded region could then be calculated. The fatigue damage and the remaining fatigue life in the region could be analyzed correspondingly. The proposed FE model should be adequate to calculate the normal stress history and/or internal forces in the relative elements adjacent to the regions for hot-spot stress analysis. In the deck of the TMB, almost all the structural members are welded together, so the elements were meshed at the corresponding connected points. On the other hand, considering the limit of the computational cost, the element meshes in the FE model could not be too fine. In the established TMB FE model, a practical structural member was just modelled as an element. For instance, a diagonal bracing or a vertical post was modelled as an I-beam element. The chords and the cross-frames were modelled at the relative connected points of the structural members. Fig. 2 shows the FE model of a typical deck unit. The spatial configurations of the original structure are retained in the model. More than 7300 nodes and 19 000 elements are included in the TMB FE model.

3. Verification of the model

The modal properties of the TMB under free vibration and its dynamic stresses under the train loading were studied with the developed FE model. Comparison of the computed results with the measured data was used to verify the efficiency of the FE model.

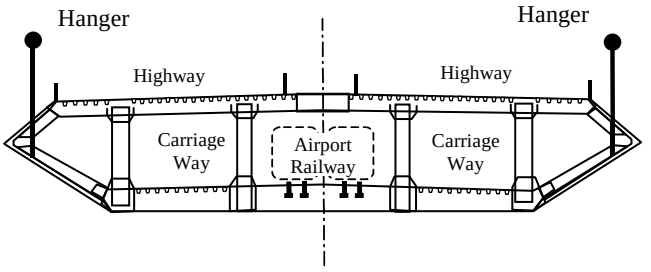

(a) Typical Cross Section of the Bridge Deck

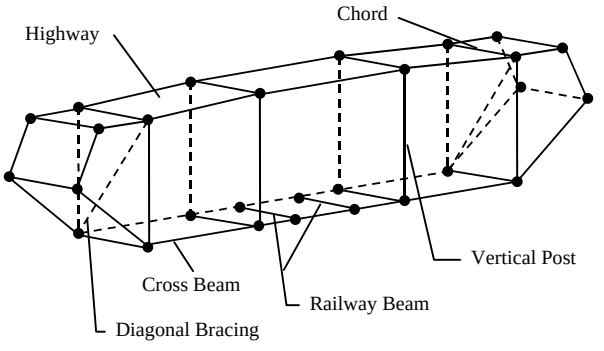

(b) Nodes and Elements in the FE Model of a Bridge Unit Deck

Fig. 2. Cross-section of the bridge deck and FE model.

3.1. Modal properties

The Eigenvalue problem for the natural modes of a FE model [14] is

$$(\mu^2[M] + \mu[C] + [K])\{\phi\} = 0, \tag{1}$$

where $[M]$ is the mass matrix, $[C]$ is the damping matrix, $[K]$ is the stiffness matrix, which may include large-displacement effects, such as "stress stiffness" (initial stress terms), μ is the eigenvalue, and $\{\phi\}$ is the eigenvector. During eigenvalue extraction in ABAQUS, the damping was neglected. When the eigenvalue $\bar{\mu}$ without damping is calculated, the eigenvalue with damping is, $\mu = \bar{\mu}\sqrt{1 - c^2}$.

In the eigenvalue calculation, the initial stress in the hangers and main cables must be considered carefully because the initial stress greatly affects the structural stiffness matrix [15]. The initial stresses were tested when the bridge was just constructed, and were adopted as the stress initial conditions in the FE model.

The periods of the first 80 modes of free vibration were computed with FEM ranging from 2.305 to 0.134 s. Some free-vibration frequencies were measured separately by the Tsing Hua University (THU) in China, the Hong Kong Polytechnic University (HK PolyU) and the Hong Kong Highways Department (HKHD). The designer Mott MacDonald Hong Kong Ltd. (MMHK) and the checker Flint & Neill Partnership of UN (FNP) of TMB also analyzed

Table 1
Few free-vibration frequencies of TMB, unit (Hz)

Mode	MMHK	FNP	THU	HK PolyU	HKHD	Mean	FEM	Difference (%)
Lateral								
First	0.065	0.064	0.069	0.069	0.070	0.0674	0.069	+2.3
Second	0.164	0.149	0.161	0.164	0.170	0.1616	0.161	−0.4
Vertical								
First	0.112	0.112	0.114	0.113	0.114	0.1130	0.117	+3.4
Second	0.141	0.133	0.137	0.139	0.133	0.1366	0.144	+5.1
Torsion								
First	0.259	0.253	0.265	0.267	0.270	0.2592	0.262	+1.1
Second	0.276	0.268	0.320	0.320	0.324	0.3016	0.332	+9.2

theoretically the first few frequencies [16]. Table 1 gives a comparison between the first few measured and analytical natural frequencies.

In Table 1, the "mean" data in the seventh column are the mean values of frequencies of the second to sixth columns, which include measured and theoretically results. The difference $=(FEM - Mean)/FEM * 100\%$. The maximum relative difference is 9.2%, which shows that the frequencies calculated by the constructed FE model compare well with the measured and the analyzed ones. The main dynamic response properties are included in the FE model. It is efficient to study the modal properties of the TMB using the FE model [17].

As a matter of interest, the first lateral, vertical and torsion modes of the bridge are shown in Figs. 3–5, respectively. In the figures, the x direction is allocated along the bridge longitudinal direction, the y direction is vertical, and the z direction is in the bridge lateral direction. Each mode shape is depicted with respect to main cables (and towers) in x–z and x–y planes, and with respect to deck longitudinal girders in $x-z$ and $x-y$ planes. In these figures, the legend "original" denotes the static configuration of the bridge; the legend "cable 1" indicates the modal motion of the front cable with $z = +18.0$ m; the legend "cable 2" indicates the modal motion of the back cable with $z = -18.0$ m; the legend "chord 1" indicates the modal motion of the front longitudinal bottom chord with $z = +13.0$ m; and the legend "chord 2" indicates the modal motion of the back longitudinal bottom chord with $z = -13.0$ m.

3.2. Comparison of the computed stress responses with the monitoring data

The effectiveness of the FE model was studied before it was used to analyze the dynamic response of the TMB. The TMB carries both highway and railway traffic. Relatively, its dynamic response is caused by the combination of truck or highway loading and train loading. The truck loading is very complex because it varies with traffic flow, vehicle types, the road roughness and the vehicles' lateral positions, etc. There are many uncertainties in the truck-loading model. Conversely, a train has fixed axle spacings and known axle loading. The train-loading model is more reliable in this sense than the truck-loading model. Being the first step of the research, the dynamic response of the bridge under a running train was considered.

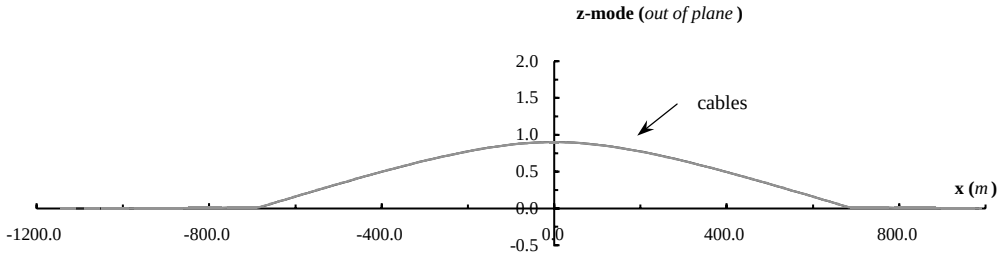

(a) Modal motion in cables

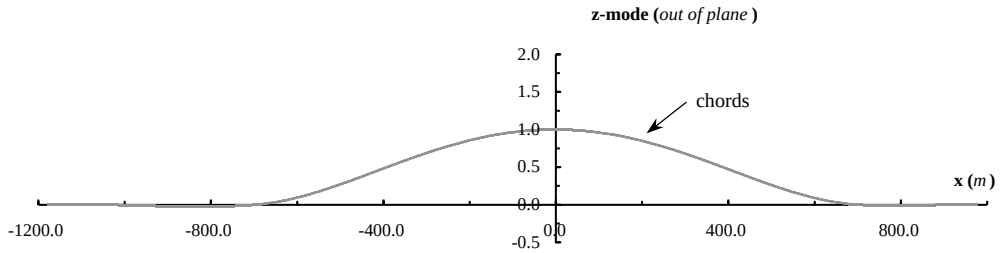

(b) Modal motion in deck

Fig. 3. The first lateral vibration mode.

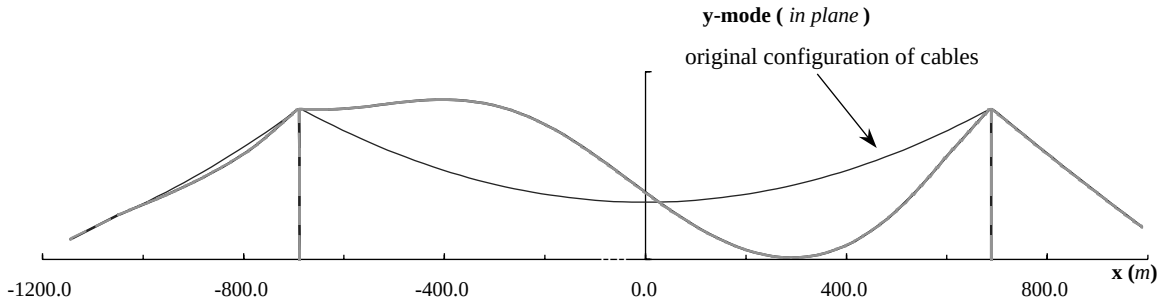

(a) Modal motion in cables

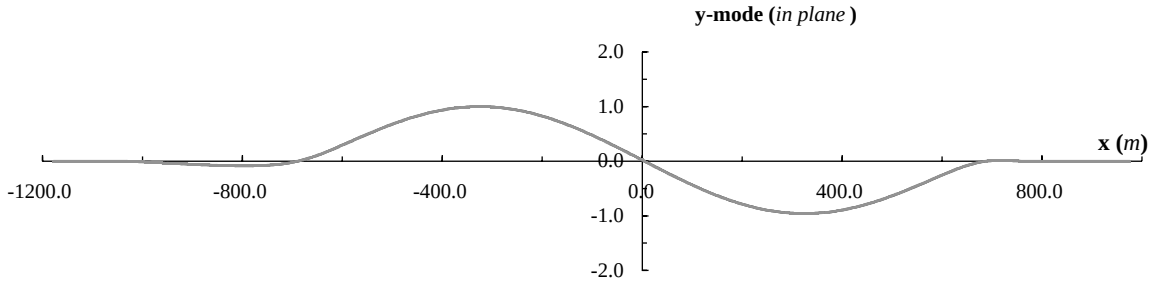

(b) Modal motion in deck

Fig. 4. The first vertical vibration mode.

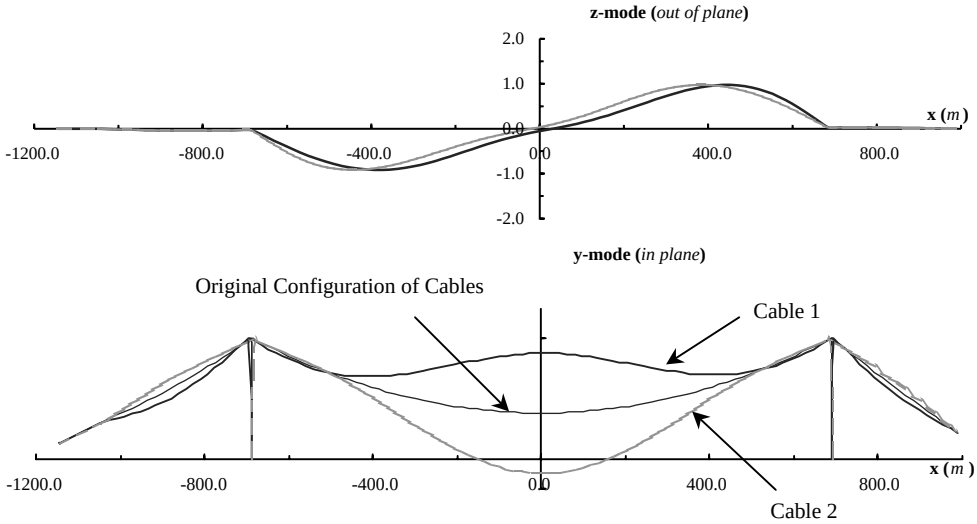

(a) Modal motion in cables

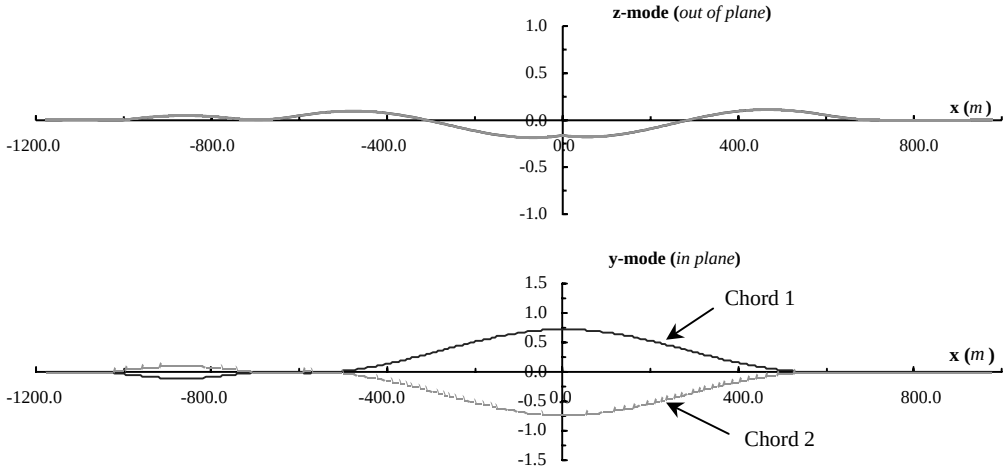

(b) Modal motion in deck

Fig. 5. The first torsional vibration mode.

When a train passes across a bridge, periodic excitations can be induced to generate bridge deformation, and bridge fatigue damage can then be produced. For a long-span bridge–train system, Diana and Cheli [18] pointed out that the interaction between the train and bridge should be considered while studying the bridge deformation. Recently, Xia et al. [19] established an accurate train–bridge model to study the dynamic interaction of long-suspension bridges with running trains. Their results indicated that the dynamic interaction between the train and long-span bridge is insignificant. To avoid the model being more complicated, the running train is simulated as moving loads in the established model. When the speed of the moving load is very

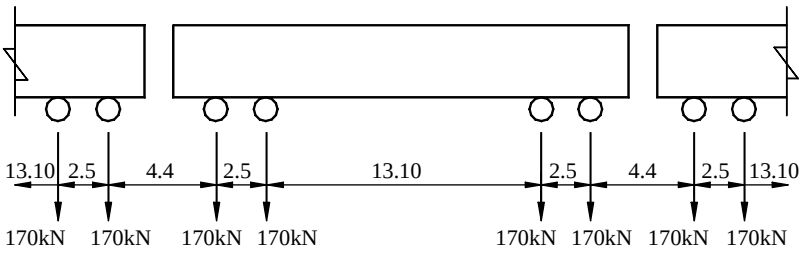

Fig. 6. Configuration of a train, unit (m).

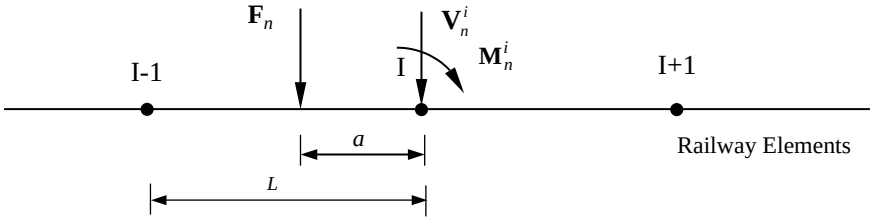

Fig. 7. Railway living loading and nodal forces.

slow, the crawling speed load can be considered as a static load, and the corresponding response as the influence line of the response. Work by Moses et al. [20] indicated that the impact factor of a long-suspension bridge would not be over 10%. Therefore, the moving load model is accurate enough to study the bridge response under running trains.

A typical train model [19] is shown in Fig. 6: each axle loading of the train is about 170 kN while the train is fully loaded. A train with 10 cars full of passengers was adopted in this model. To calculate the bridge dynamic response, the equivalent nodal forces are needed.

Considering a random ith node in railway elements $(I-1, I)$ and $(I, I+1)$, the nodal force $\mathbf{V}_n^i$ and moment $\mathbf{M}_n^i$ caused by nth live axle load $\mathbf{F}_n$ (as shown in Fig. 7), is a function of ith node space location $\mathbf{x}_i$ and the axle load $\mathbf{F}_n$ local position ξ:

$$\mathbf{V}_n^i = \mathbf{V}_n^i(\xi_n, \mathbf{x_i}), \quad \mathbf{M}_n^i = \mathbf{M}_n^i(\xi_n, \mathbf{x_i}) \quad (-1 \leqslant \xi_n \leqslant 1), \tag{2}$$

where $\xi = \pm a/L$, L is the longitudinal dimension of a railway element, and a is the distance between $\mathbf{F}_n$ position and ith node along train running direction. When $|\xi_n| \geqslant 1$, the nth axle force $\mathbf{F}_n$ is not within the elements $(I-1, I)$ and $(I, I+1)$, and will not affect the ith nodal forces.

In thinking of axle load $\mathbf{F}_n$ as a live load, its position varies with time t and the train speed V_0:

$$\xi_n = \xi_n(t, V_0). \tag{3}$$

While a train is running on the bridge, the nodal forces at ith node are the total equivalent forces caused by all axle forces of a train, i.e.,

$$\mathbf{V}_i = \sum_n \mathbf{V}_n^i(\xi_n(t, V_0), \mathbf{X}_i), \quad \mathbf{M}_i = \sum_n \mathbf{M}_n^i(\xi_n(t, V_0), \mathbf{X}_i). \tag{4}$$

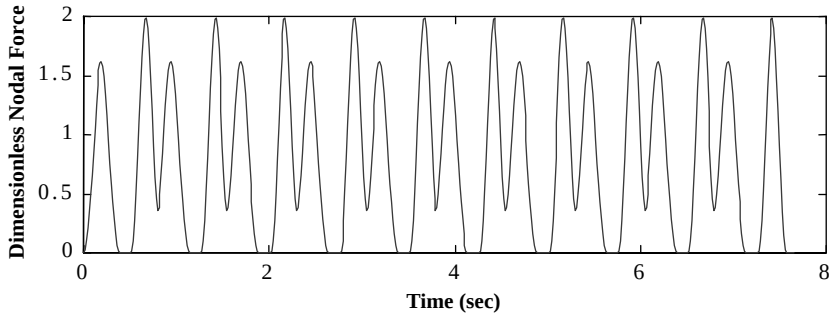

(a) Nodal Forces

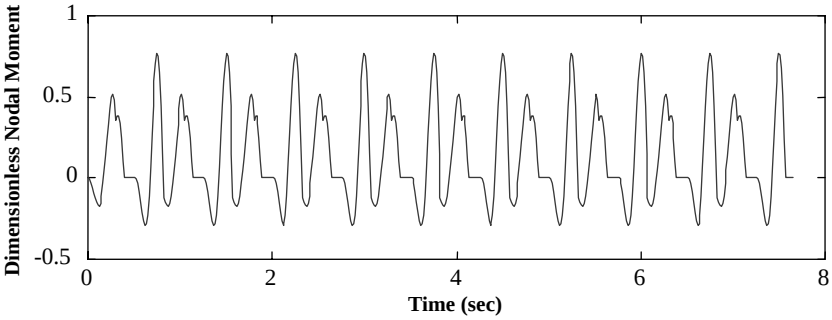

(b) Nodal Moments

Fig. 8. Equivalent nodal forces under running train loading.

With Eq. (4), typical nodal force–time and moment–time histories are shown in Fig. 8, where the train speed was considered as 30 m/s and the time was the whole period of a train axle load affecting the nodal force.

When the equivalent nodal force was added to the FE model, the dynamic response of the TMB was analyzed. The modal superposition method was adopted to study the dynamic response. As long-suspension bridges bear global deformation at very low frequency and local deformation at relatively high frequency, assuming the bridge local deformation to be included in the response, the first 80 modes were selected in the analysis. The effective masses are more than 93% of the total masses when the first 80 modes were used in the dynamic analysis; therefore, the number of modes is enough for dynamic analysis. Additionally, considering that long-suspension bridges are lightly damped structures, the modal damping was chosen as 0.5% in the FEM.

Comparison of the computed results with the measured online data was needed to validate the efficiency of the FEM. The online dynamic response of the TMB was measured by a structural health monitoring system permanently installed on the bridge. Forty-seven strain gauges were installed on the frame CH-24662.5 to measure the strain–time history. Some typical locations of strain gauges are shown in Fig. 9.

Generally, the measured strain–time data is the response of the bridge under both rail loading and truck loading, but the computed results are the response just under rail loading. In normal conditions, it is not easy to take a control test to measure the bridge dynamic response under rail loading only. Occasionally, the highway on the bridge will be closed, but the railway will still be

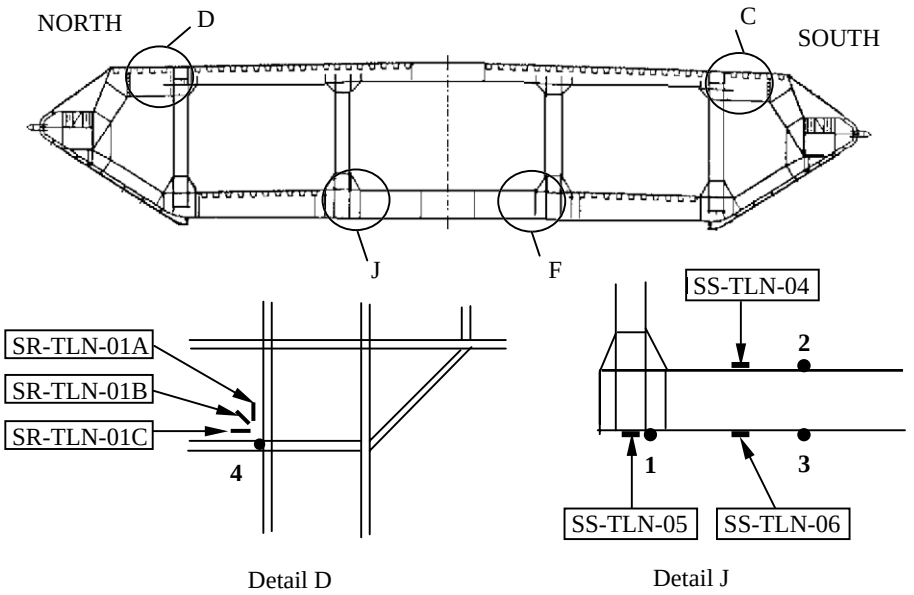

Fig. 9. Typical locations of strain gauges in the bridge deck.

opened under some emergent conditions, e.g. when the bridge is attacked by a typhoon. On September 16, 1999, typhoon York directly hit Hong Kong and the highway on the TMB was closed. The eye of York was closest to the TMB at 10 a.m. that day. Within a typhoon eye, there is almost no wind effect to the structure. During the 2 h taken for the eye of York to get past the TMB, given that hardly any vehicle traffic passed along the bridge, the TMB could reasonably be considered to be under train loading only. The measured data from 10 a.m. to 11 a.m. were selected for comparison with the computed results.

The strain–time history selected from the online data recorded by the strain gauges (as shown in Fig. 9) located at detail "D" and detail "J" were considered, where the strain gauge "SR-TLN-01" is a strain rosette, and the corresponding principle stresses in the location were computed for comparison. Because the TMB is symmetrical about the bridge centerline, the strain–time histories recorded by the strain gauges in details "C" and "F" are similar to those in details D and J, and were not studied separately. With the strain–time-history data, the stresses versus time in the locations could be obtained easily using Hooke's law (where Young's modulus is 200 GPa), and are shown in Fig. 10.

Each sudden change in the curves corresponds to the passage of a train. Obviously, there were eight trains which had passed through the TMB during the hour of interest, four of which were airport-bound and vice versa. When trains passed through the bridge in different directions, the differences of the responses at "SS-TLN-04" and "SS-TLN-05" were very distinct. In the developed FE model, the bridge responses under an airport-bound train were simulated and correspondingly compared to the measured data in the same train direction.

A comparison between the computed results and the measured data was carried out. To be more distinct, the related stresses due to the passage of a train were selected. The stresses should not be compared with the computed results directly because the measured stresses are affected by

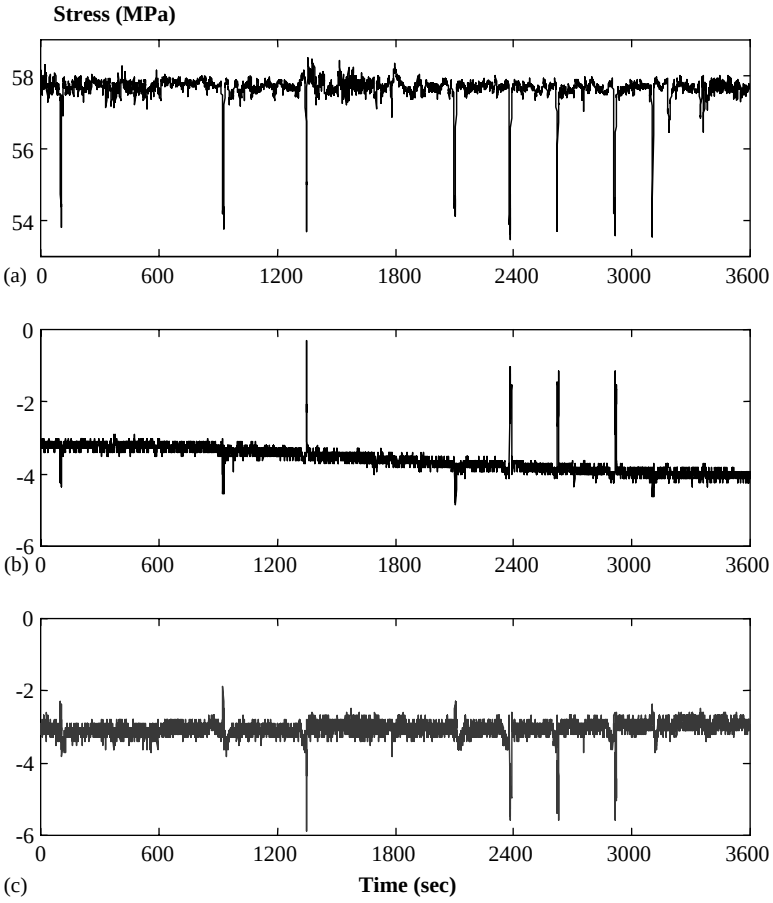

Fig. 10. Measured stress–time histories at: (a) SR-TLN-01, (b) SS-TLN-04, (c) SS-TLN-05.

many factors, including traffic loading, temperature change, and the initial conditions during the installation of the strain gauges. However, being the most important factor to cause structural fatigue damage, the stress fluctuation is mainly caused by traffic loading [11]. The stresses recorded by strain gauges should be calibrated for comparison with the computed data, i.e., the selected stress peak should be moved to locate at the same time as the computed data, and the measured stress value to be equal to the computed datum at time zero. The relevant stress response output points are shown in Fig. 9. The comparison of output stresses at points "4", "1" and "2" with the recorded data by SR-TLN-01, SS-TLN-05 and SS-TLN-04 are shown in Fig. 11.

As shown in Fig. 11, there is just a stress cycle within the passage of a train by FE analysis. However, with the measured data, there is a main block stress cycle that consists of some small stress cycles. The small stress cycles reflect the local dynamic response of the bridge and correspond to much higher modes that cannot be included in the limited modal superposition analysis. However, in the analysis of high-cycle fatigue damage, the main stress cycle is most

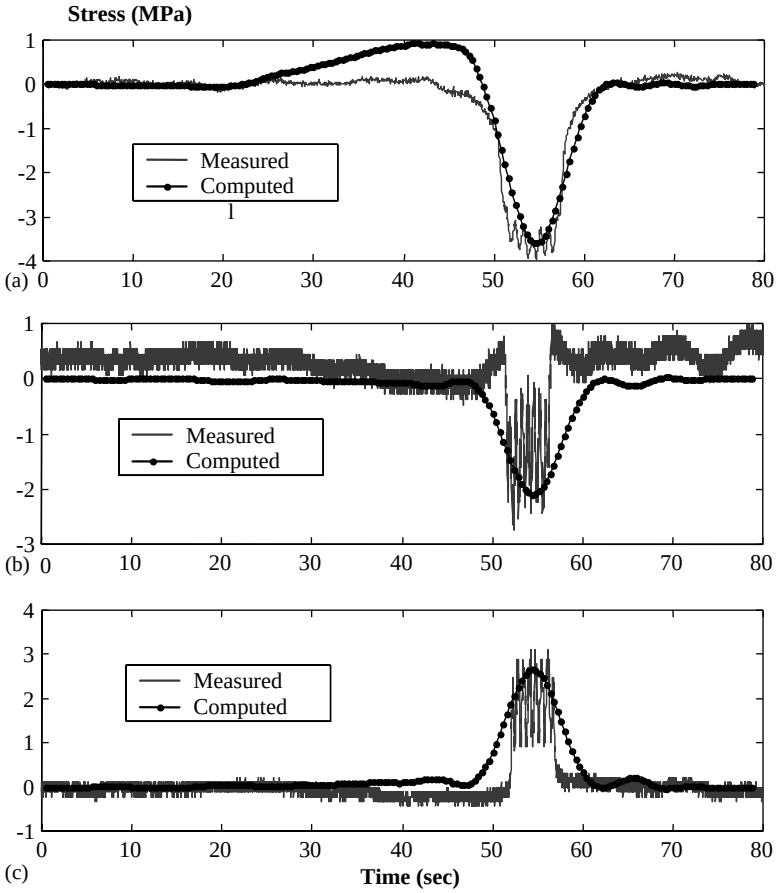

Fig. 11. Comparison of computed stress histories with measured ones at: (a) SR-TLN-01, (b) "SS-TLN-05", (c) "SS-TLN-04".

important and the small stress cycle can be neglected. Fig. 11 shows that the computed stress spectrum compared well with the recorded data.

From the aforementioned comparison of the computed results by the developed FE model with the measured data, it could be seen that the model could be used to study the dynamic response of the bridge for fatigue analysis.

4. Dynamic response of the TMB under traffic loading

In the case of bridges carrying both highway and railway loadings, the total fatigue damage should be determined for each loading condition separately [3]. Because there is only a single rail track passing through the TMB in each direction, the additional combined stress history by more than two trains could be neglected. The computed stress history (see Fig. 11) should be used directly to calculate the fatigue damage in the TMB. With the volume of train passages in a block

(i.e., the stress cycle numbers in a block due to train loadings should be known) [12], using the Palmgren–Miner rule [3], the fatigue damage under train loadings in a block could be obtained.

In British standards, individual truck passages were considered to control fatigue behavior for short- and medium-span bridges. However, it would not be appropriate to simply adopt the same procedure in a fatigue evaluation for long-span bridges. As discussed by Moses et al. [20], the effect of groups of trucks is very important to such bridges' fatigue behavior. The TMB carries a double three-lane highway. To study the fatigue damage due to highway loading, the combined stress history under vehicles in the same direction should be studied.

As mentioned earlier, it is more complicated to study the dynamic response of the bridge under truck loading than under train loading. In addition, when a truck was running on the bridge, the local response of the bridge was dominant and a much higher modal state was activated. It was still not convergent when 120 modals were adopted to calculate the bridge response under truck loading. Therefore, the modal superposition method is unsuitable for studying the bridge dynamic response caused by trucks. Here, the direct implicit integration method was adopted to compute the response. However, it is still too expensive to compute the bridge dynamic response in the whole process of a truck passing through the bridge. In normal conditions, the affected time in an element with a passage of a truck is less than 2 s, which could be found in a typical stress–time history curve from online data, as shown in Fig. 13(a).

To calculate the stress–time history caused by highway loading in an element, only the period of a truck affecting the element was considered. Correspondingly, the computing time was significantly reduced. It is an efficient way to compute the bridge local response.

Computed stress–time histories at CH24662.5 under a single truck are depicted in Fig. 13(b), where the truck is a standard British fatigue truck [3] running in the shoulder lane (as shown in Fig. 12(a)), and its speed is chosen as 25 m/s. As shown in Fig. 13(b), the measured affecting time of an element accords well with the computed result. However, the stress spectra could not be compared because the axle load and configuration of the corresponding truck and its lateral location on the bridge could not be determined accurately.

As the affected time of an element under a truck passage is less than 2 s (as shown in Fig. 13) and the space between the two trucks along their running direction in a lane is the running distance in 3 s under normal speed, the longitudinal combination of trucks in the same lane could be ignored. The lateral combination should be considered. As shown in Fig. 12, three typical lateral positions of trucks are considered. Certainly, there may be other trucks lateral distribution conditions, but the three truck-loading conditions studied here should cover most of the cases in practical highway loadings [21] that cause more serious bridge damage than other loading conditions. The corresponding computed stress histories are depicted in Fig. 14.

With the calculated stress histories under the above traffic loading conditions, as well as with the statistical truck volumes in a block time under the three loading conditions from WIM data, the fatigue damage caused by truck loading could be obtained.

The stress analysis here provides a base for studying the bridge fatigue damage. To obtain the total damage under the railway and highway loadings, the probability of co-existence of the two types of loading should be taken into account. The fatigue damage calculation will be reported in a separate paper.

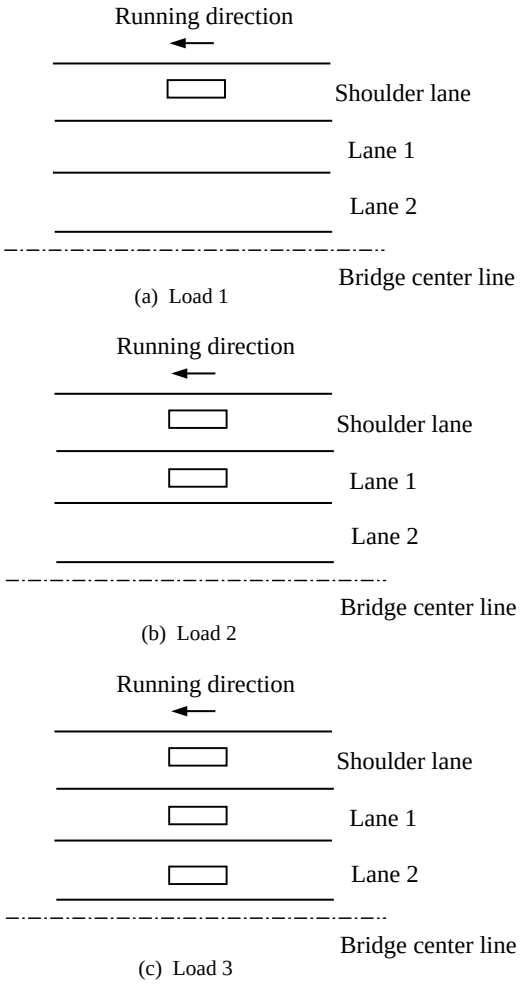

Fig. 12. Truck lateral positions on the bridge deck.

5. The critical fatigue location in the TMB

It is significant to decide the critical locations due to fatigue damage in practical bridges. In the aforementioned stress analysis, the bridge responses under highway loading and under railway loading were studied separately. The critical location due to fatigue damage under these two types of loading could then be analyzed.

The computed bridge response under truck loading is just the local response at CH24662.5. The stress distribution in the elements around CH24662.5 is depicted in Fig. 15(a). From Fig. 15(a), it can be seen that the critical locations are the outmost part of the upper chord and the bottom cross-frame between the rail tracks. In considering the limited computational cost, the whole process of a truck passing through the bridge would not be computed with the direct implicit integrate method. To know about the local response under traffic loading

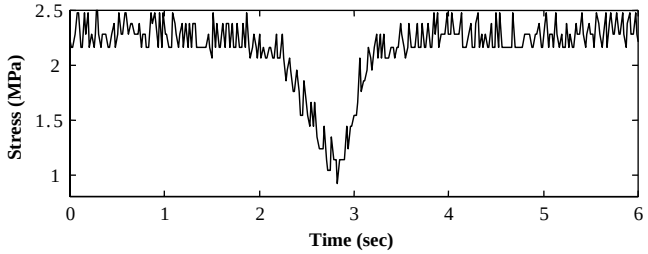

(a) Measured Stress versus Time under Truck Loading

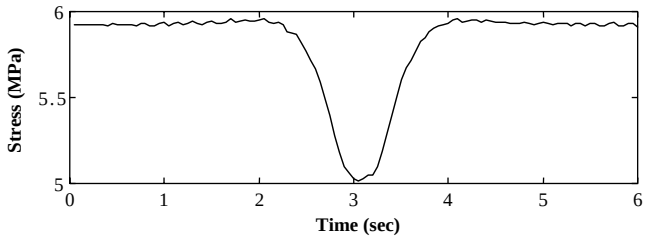

(b) Computed Stress versus Time under Truck Loading (Load 1)

Fig. 13. Stress versus time under truck loading.

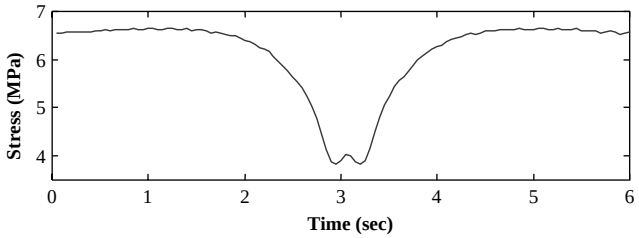

(a) Under Load 2

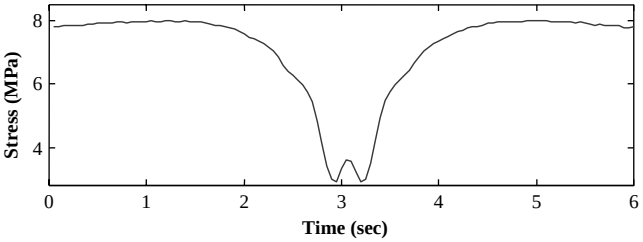

(b) Under Load 3

Fig. 14. Computed stress versus time under truck loading.

along the bridge longitudinal direction, the responses of the elements around CH24311.5, which is around the middle of the main span, are computed. The stress-contour distribution in the relative elements is shown in Fig. 15(b). Comparison of Fig. 15(b) with Fig. 15(a)

shows that the critical locations due to fatigue damage are at similar locations at each chainage.

The critical locations due to fatigue damage under rail loading were also identified. The stress contour distribution in the elements around CH24662.5 under train loading is depicted in Fig. 16. From Fig. 16, the critical locations in the deck unit are at the outmost part of the upper chord, which is similar to the critical locations under truck loading. The stress distributions in other deck units are similar to ones at CH24662.5.

As the local responses under truck loading are similar, the critical locations due to fatigue damage in the whole main span are mainly decided by rail loading. When a train passed through the TMB along the outbound airport track, the stress spectra in the outmost of the upper chords along the bridge longitudinal direction were studied to determine the fatigue critical locations in the whole bridge.

The stress spectra in the left outmost part of the upper chords along the main span are depicted in Fig. 17. The y-axis denotes the dimensionless stress spectra, which equals $\Delta\sigma$, the stress spectrum in the focused location divided by $\Delta\sigma^*$, the stress spectrum in the chord outmost at CH24662.5. Obviously, the critical location is not at the CH24662.5, where the strain sensors were installed. Fig. 17 shows that the stress spectra in many frames are higher than the one in the frame at CH24662.5. The stress spectrum at CH23893 is about 1.2 times the stress spectrum at CH24662.5. To analyze the fatigue damage in the TMB, the stress spectrum in this location will be adopted and the remaining life of this location would be simulated.

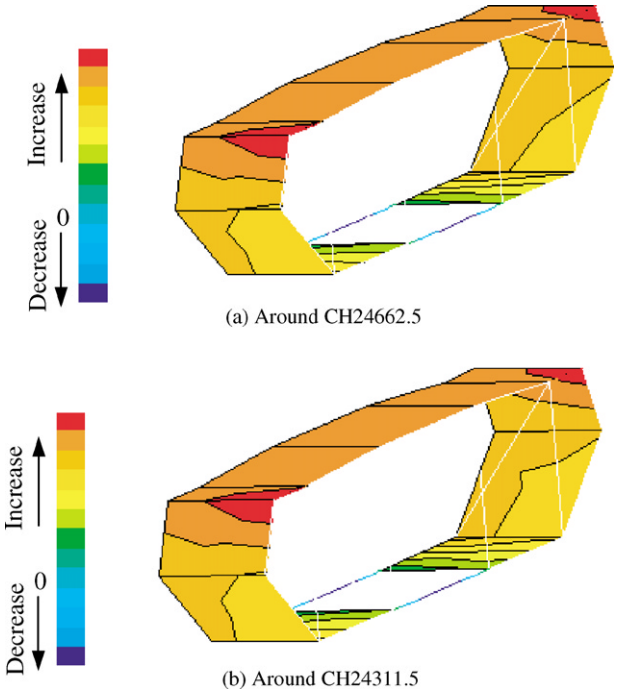

Fig. 15. Stress distributions in the elements under single truck loading.

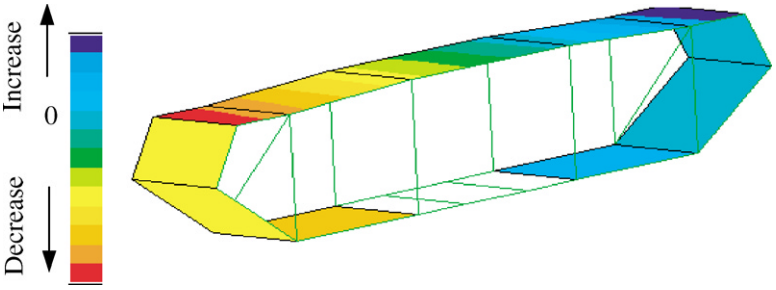

Fig. 16. Stress distributions in the elements around CH24662.5 under railway loading.

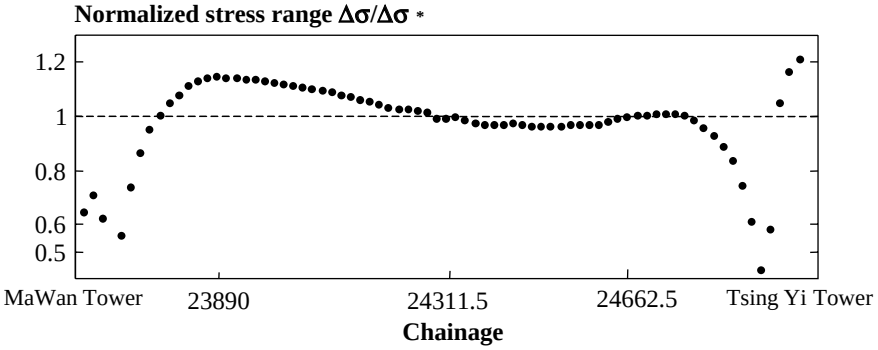

Fig. 17. Stress range along the main span of the TMB.

6. Local FE model for fatigue stress analysis

As the welded regions are vulnerable to fatigue damage, an efficient FE model for fatigue analysis should be used to output the stress at these locations. However, the aforementioned global stress analysis just could obtain the normal stress history in the elements around a welded location. Local FE model is proposed to calculate the hot-spot stress in the welded region for fatigue damage and the remaining fatigue life analysis.

There are some kinds of welded connections in the TMB deck. As a case of study, a typical welded connection (depicted in Fig. 18) is selected for fatigue damage analysis. In the considered joint, the longitudinal beam and vertical post are connected using fillet welds. A local FE model of considered welded connection is shown in Fig. 19 for hot-spot stress analysis. As the longitudinal beam is box section member and the vertical post is H-section member, they are all modelled as shell elements. In thinking of the hot-spot stress must include all the stress-concentrating effects of the welded detail, the region around the welded connection are modelled as 3-D brick elements. The connecting conditions between the shell elements and brick elements are accommodated through a series of penalty elements [22].

The normal stress history and/or internal forces in the relative elements adjacent to the welded connection, which were obtained through the aforementioned global stress analysis, are considered as the external forces in the presented local FE model. Fig. 20 gives the hot-spot stress distribution in the welded connection under a train loading. From the stress distribution

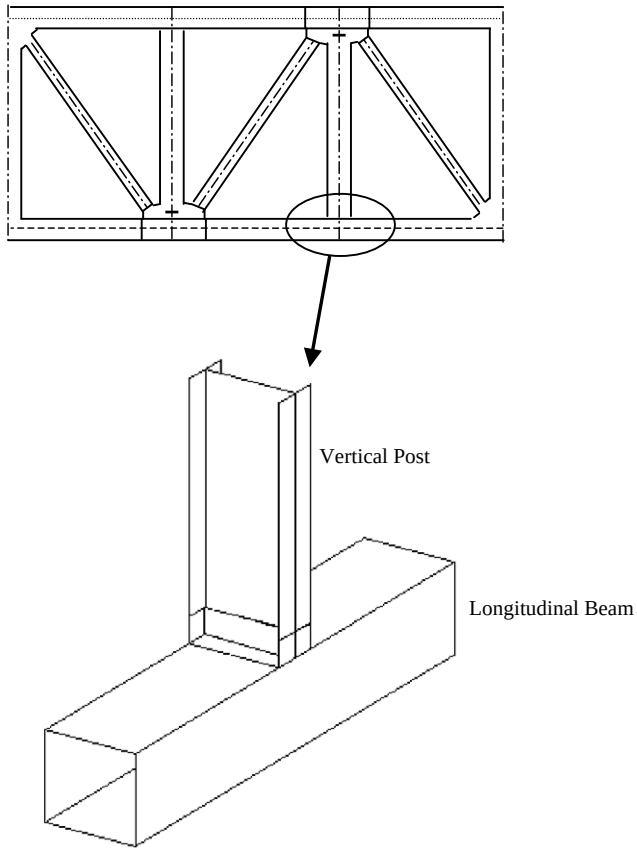

Fig. 18. Typical welded connection in the TMB deck.

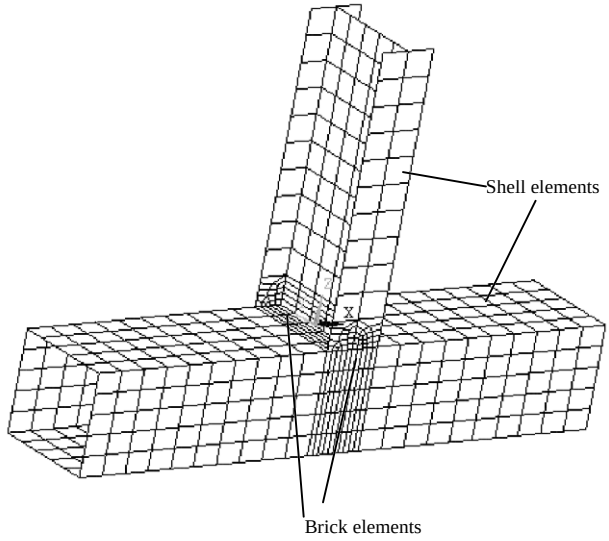

Fig. 19. Local FE model of the typical welded connection.

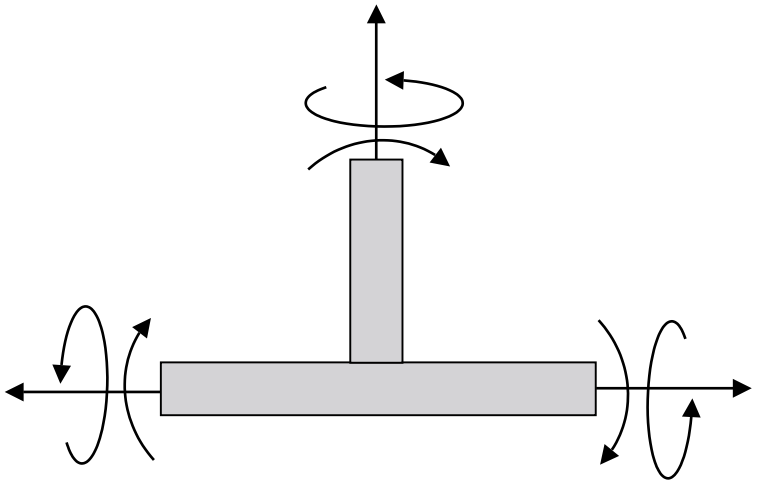

(a) External forces in the connection

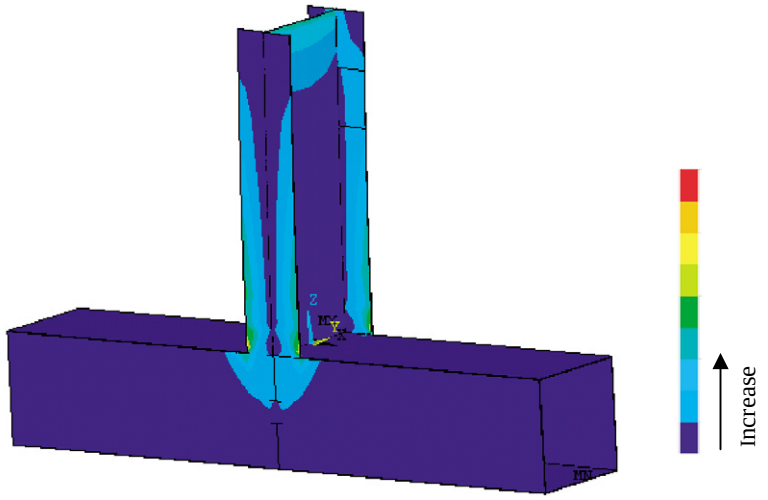

(b) Hot-spot stress distribution in the connection

Fig. 20. Hot-spot stress analysis of a typical welded connection.

figure, it is easy to see that the hot-spot stresses in the welded region are much higher than the normal stress. From the analysis results, the fatigue damage degree in the locations could be computed and the remaining life of the bridge could then be evaluated, which will be discussed in more details in a separate paper.

7. Conclusions

A large FE model of a long-suspension bridge was developed in this paper. In order to be suitable for fatigue stress analysis, the developed FE model embodied the spatial configurations of

the original structure and weld-connection details. The verification of the model was carried out with the help of the measured data. With the comparison of the computed first few modal eigenvalues with the measured ones, the main modal properties of the TMB has been included in the developed FE model. With the developed FE model, the dynamic responses of the bridge under the running train were also studied using the modal superposition method. The computed results agree well with the online data measured by the structural health monitoring system installed on the bridge. These results show that the proposed FE model in this paper is efficient for fatigue stress analysis.

The dynamic responses of the bridge under the highway and railway loading were studied with the developed FE model. During the extraction of the bridge responses under highway loadings, the effects of groups of trucks were considered. The computed stress spectra in the bridge deck could be used for subsequent fatigue damage analyses.

Critical fatigue locations within the bridge main span were also decided by FE analysis. In any cross-frame, the elements at the two outmost of the upper chord are more critical to fatigue damage. Along the main span, the critical fatigue locations do not have any strain sensors installed.

All the above results provide the basis for evaluating fatigue damage in the bridge and predicting its remaining service life. The developed FE model could also be used to simulate the dynamic response of the bridge under some disastrous conditions.

Acknowledgements

Funding support for this project by the Research Grants Council of the Hong Kong SAR Government (Project code: Polyu 5042/01E), the Hong Kong Polytechnic University and the National Natural Science Foundation of China (No. 50178019) are gratefully acknowledged. Appreciation is extended to the Highways Department of the Hong Kong SAR Government, which provided the data measured by the health monitoring system and relevant documents.

References

[1] ASCE, Committee on fatigue and fracture reliability of the committee on structural safety and reliability of the structural division, fatigue reliability 1–4, Journal of Structural Engineering 108 (1982) 3–88.
[2] R.A. Barrish, A.K. Grimmelsman, A.E. Aktan, Instrumented monitoring of the Commodore Barry Bridge, Proceedings of SPIE, Nondestructive Evaluation of Highways, Utilities, and Pipelines IV, Vol. 3995, 2000, pp. 112–126.
[3] BSI, BS5400: Part 10, Code of Practice for Fatigue, 1982.
[4] R. Pullin, D.C. Carter, K.M. Holford, Damage assessment in steel bridges, Key Engineering Materials 167–168 (1999) 335–342.
[5] W.R. Charles, M. Gregory, C. Paul, A. Kayoko, W. Scott, Dynamic response and fatigue of steel Tied-Arch Bridge, Journal of Bridge Engineering 5 (2000) 14–21.
[6] H. Nowack, U. Schulz, Significance of finite element methods in fatigue analysis, G. Lutjering, H. Nowack (Eds.), Fatigue 96: Proceedings of the 6th International Fatigue Conference, Vol. 2, Pergamon, Oxford, 1996, pp. 1057–1068.

[7] I.V. Putchkov, Development of a finite element based strain accumulation model for the prediction of fatigue lives in highly stresses Ti components, International Journal of Fatigue 17 (1995) 385–398.
[8] X.B. Lin, R.A. Smith, Finite element modeling of fatigue crack growth of surface cracked plates, Part I: the numerical technique, Engineering Fracture Mechanics 63 (1999) 503–522.
[9] X.B. Lin, R.A. Smith, Finite element modeling of fatigue crack growth of surface cracked plates, Part II: crack shape change, Engineering Fracture Mechanics 63 (1999) 523–540.
[10] X.B. Lin, R.A. Smith, Finite element modeling of fatigue crack growth of surface cracked plates, Part III: stress intensity factor and fatigue crack growth life, Engineering Fracture Mechanics 63 (1999) 541–556.
[11] T.H.T. Chan, Z.X. Li, J.M. Ko, Analysis and life prediction of bridges with structural health monitoring data—Part II: application, International Journal of Fatigue 23 (1) (2001) 55–64.
[12] Z.X. Li, T.H.T. Chan, J.M. Ko, Fatigue analysis and life prediction of bridges with structural health monitoring data—Part I: methodology and strategy, International Journal of Fatigue 23 (1) (2001) 45–53.
[13] ABAQUS/Standard User's Manual, Version 5.8, Hibbitt, Karlsson and Sorensen, Inc., Pawtucket, RI, 2000.
[14] J.H. Wikinson, The Algebraic Eigenvalue Problem, Oxford University Press, Oxford, 1965.
[15] K.J. Bathe, Finite Element Procedures in Engineering Analysis, Prentice-Hall, Englewood Cliffs, NJ, 1982.
[16] C.K. Lau, W.P. Mak, W.Y. Chan, K.L. Man, K.F. Wong, Structural performance measurements and design parameter validation for Tsing Ma Suspension Bridge, Advances in Steel Structures ICASS '99, Hong Kong, 1999, pp. 487–496.
[17] J.Y. Wang, J.M. Ko, Y.Q. Ni, Modal sensitivity analysis of Tsing Ma Bridge for structural damage detection, Nondestructive Evaluation of Highways, Utilities, and Pipelines IV, Proceedings of SPIE, Vol. 3995, 2000, pp. 300–311.
[18] G. Diana, F. Cheli, Dynamic interaction of railway systems with large bridges, Vehicle System Dynamics 18 (1989) 71–106.
[19] H. Xia, Y.L. Xu, T.H.T. Chan, Dynamic interaction of long suspension bridges with running trains, Journal of Sound and Vibration 237 (2000) 263–280.
[20] F. Moses, C.G. Schilling, K.S. Raju, Fatigue evaluation procedures for steel bridges, National Cooperative Highway Research Program Report 299, Washington, DC, 1987.
[21] M.P. Enright, D.M. Frangopol, Reliability based lifetime maintenance of aging highway bridges, Proceedings of SPIE, Nondestructive Evaluation of Highways, Utilities, and Pipelines IV, Vol. 3995, 2000, pp. 4–13.
[22] L. Guo, T.H.T. Chan, Z.X. Li, Fatigue damage analysis of large suspension bridge using finite element method, Journal of Engineering Structure, submitted for publication.